学位論文（博士）

Quantification of pancreas fat on dualenergy computed tomography: comparison with six-point Dixon magnetic resonance imaging.

(Dual energy CT による膵臓の脂肪定量化：six-point Dixon MRI と比較検討)

氏名　亀田　ふみ

所属　山口大学大学院医学系研究科

医学専攻　放射線医学講座

令和２年１１月

学位論文の関連論文の研究背景及び要旨

所属　放射線医学
氏名　亀田　ふみ

〔題名〕

Quantification of pancreas fat on dual-energy computed tomography: comparison with six-point Dixon magnetic resonance imaging.

（Dual energy CT による膵臓の脂肪定量化：six-point Dixon MRI と比較検討）

Abdominal Radiology, volume 45, p2779–2785(2020)

〔研究背景〕

内臓脂肪組織は、メタボリックシンドロームや心血管疾患の発症の危険因子として知られている。膵臓では膵脂肪沈着と 2 型糖尿病との関連が報告されており、膵内分泌機能の予後を推定するため、画像診断によって非侵襲的かつ正確に膵内脂肪量を定量化することは臨床的に有用と考えられる。しかしながら従来の CT では膵内脂肪量を定量化することは困難であった。一方、MRI は組織脂肪含有量の定量化に優れており、特に six-point Dixon 法 MRI などのケミカルシフトイメージングや MR スペクトロスコピーは、肝臓や膵臓などを含む様々な臓器で組織脂肪定量の精度の高さが研究で明らかになっている。

Dual energy CT(以下 DECT)は 1 種類の管電圧で撮影される CT と異なり、2 種類の管電圧を使用することで、一度の撮影で 2 種類の X 線エネルギーのデータを取得することができる。DECT では 30%未満の肝脂肪量を評価できることが報告されており、膵内脂肪量の評価も有用と思われた。しかし、過去に膵脂肪量の定量化について MRI と DECT を比較した報告はなかった。

この研究は DECT により膵実質の脂肪含有率を測定し、six-point Dixon 法 MRI における脂肪定量画像で測定された脂肪含有率と比較することで、DECT による膵脂肪定量化の実行可能性を検討することを目的とする。

〔要旨〕

方法：

2017 年 11 月から 2018 年 12 月にかけて、当院で DECT を撮影した患者で、腹部 MRI(fat fraction imaging)を撮影した 28 症例を対象とした。性別は男性 18 名、女性 10 名。年齢幅は 49-84 歳であり、平均年齢は 69.4 歳であった。基礎疾患は肝細胞癌 12 名、転移性肝腫瘍 7 名、胆管癌 3 名、胆嚢癌 3 名、膵臓疾患 2 名、総胆管結石 1 名。3 ㎝以上の膵臓腫瘍 1 名、高度膵萎縮 1 名、膵臓腫瘍の外科的切除歴 1 名、また画質が不十分な患者 3 名は除外した(図 1)。

DECT と MRI の撮影は 30 日以内に実施された。

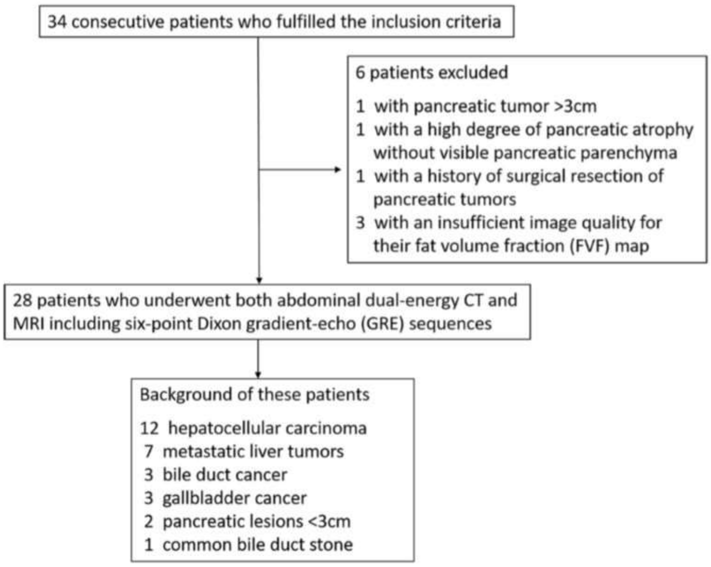

図 1 フローチャート

DECT は dual-source CT scanner（SOMATOM FORCE; Siemens, Forchheim, Germany）、MRI は 3.0T MR システム（Magnetom Prisma; Siemens Healthcare, Erlangen, Germany）を使用して撮影した。すべての画像は、画像アーカイブ通信システム（PACS）ワークステーション（Shade Quest, Yokogawa Medical）上で 2 人の放射線科医（経験年数 6 年、30 年）が評価を行った。

DECT で撮影した画像から fat map を作成し、膵頭部と体尾部各 1 か所に region of interest(ROI)を設定し計測した。ROI のサイズは円形 90－100mm2 程度、膵臓の形態に合わせて調整し、ROI の位置は画像上判別できる血管や主膵管を含まない位置を選択した(図 2)。MRI で CT と同じ部位に ROI を設定し(図 3)、計測。DECT で測定した CT-FVF(%)と Dixon MRI で測定した MR-FVF(%)の関係をスピアマン順位相関係数を用いて評価した。また MR-FVF(%)と単純 100kV CT で測定した CT 値(HU)との相関をスピアマン順位相関係数で評価した。

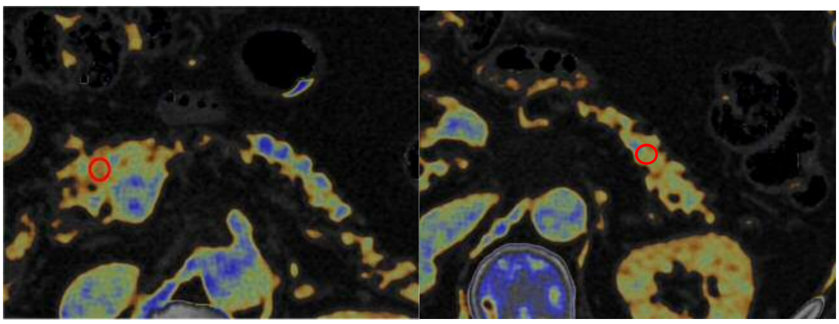

膵頭部　　　　　　　　膵体尾部

図 2　DECT 撮影画像から作成した fat map

膵頭部、体尾部に赤丸が示すように ROI を設定、CT-FVF を測定した。

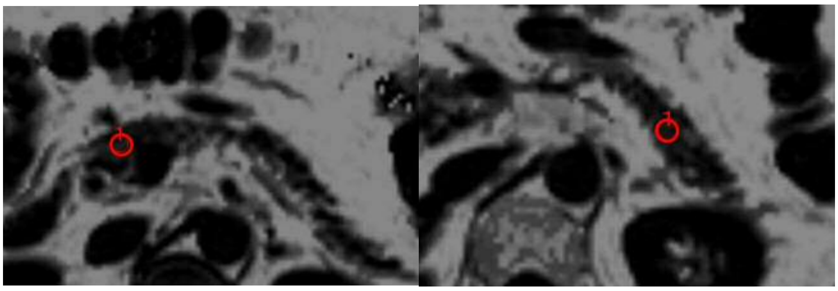

膵頭部　　　　　　　　　　　　膵体尾部

図 3　MR-FVF maps

DECT の fat map と同じ場所に ROI を設定、MR-FVF 測定した。

結果：

DECT で測定した膵頭部脂肪含有率は 14.2% (範囲 0.1-81.2%)、膵体尾部は 9.4% (範囲 0-40.8%)だった。MRI で測定した膵頭部脂肪含有率は 12.2% (範囲 1.2-80.9%) 、膵体尾部は 8.1% (範囲 0.3-43.7%)だった。DECT と MRI 測定された脂肪含有率の間には、それぞれ膵頭部 ρ = 0.631, $P < 0.001$、膵体尾部 ρ = 0.526, $P = 0.004$ の有意な正の相関関係を認めた(図 4)。

膵臓脂肪変性に対する CT-FVF 値(%)の診断能については、感度、特異度、曲線下面積(AUC)は、それぞれ頭部で 0.53、0.90、0.76、体尾部で 1.00、0.33、0.66 であった。

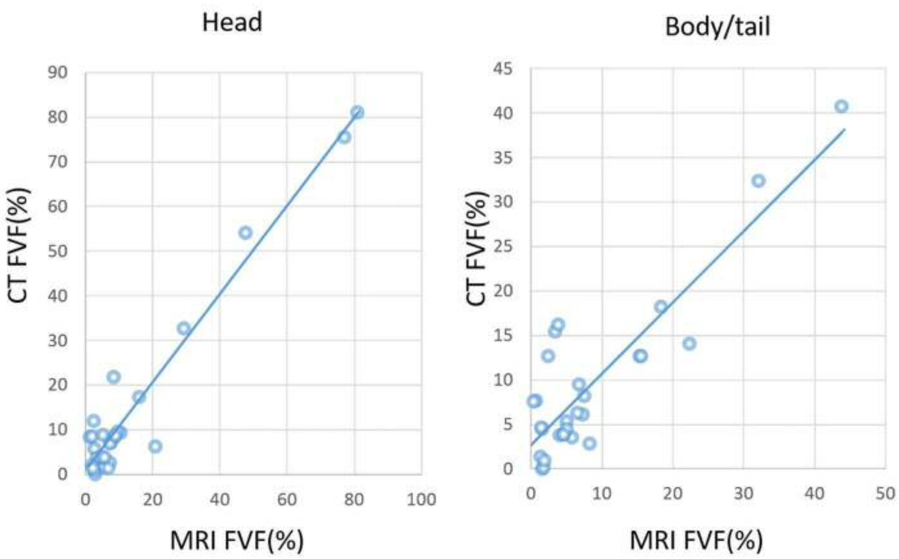

図 4　CT-CTVF(%)と Dixon MRI で測定した MR-FVF(%)

DECT と MRI 測定された脂肪含有率の間には膵頭部、膵体尾部で有意な正の相関関係を認めた。

単純 100kV CT で測定した膵頭部および体尾部の CT 値 (HU) の中央値は、それぞれ 29.5 (範囲-77.6～54.2) および 39.9 (範囲-4.4～144.8) であった。MR-FVF(%)と CT 値 (HU)との間には、膵頭、体尾部ともに有意な負の相関が認められた(頭部は ρ =-0.435、P=0.02、体尾部は ρ =-0.403、P=0.033) (図 5)。

MR-FVF(%)と CT-FVF(%)の相関および MR-FVF(%)と CT 値の相関を比較したところ、MR-FVF(%)

とCT-FVF(%)の相関のp値は、頭部(P ＜ 0.001 vs P = 0.02)と体尾部(P = 0.004 vs P = 0.033)の両方で、MR-FVF(%)とCT値の相関のp値よりも良好であった。

膵臓脂肪変性対するCT値（HU）の診断能については，感度は頭部で0.32，特異度は1.00，AUCは0.68，胴体・尾部で0.07，1.00，0.42であった。

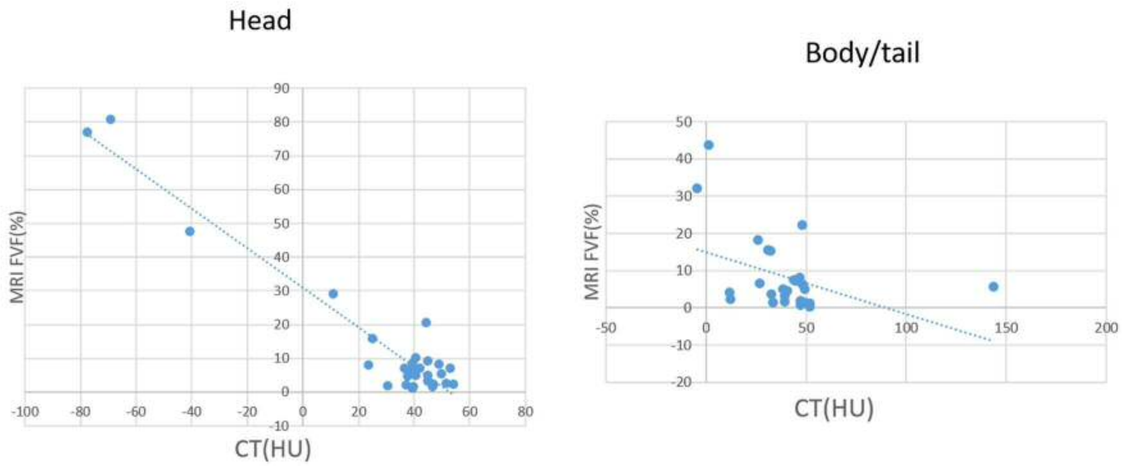

図5　MR-FVF(%)と単純100kV CTで測定したCT値(HU)

膵頭部および体尾部でMR-FVF(%)とCT値(HU)との間には有意な負の相関が認められた。

考察:

いくつかの研究では、β細胞機能障害とインスリン分泌障害の結果として、膵臓脂肪沈着が2型糖尿病の病態に関与している可能性があると報告されている。膵臓脂肪沈着は耐糖能異常の非常に初期の段階からインスリン分泌の低下と共に始まっている可能性があるとされている。

今回、脂肪定量において精度の高い手法として用いられるsix-point Dixon法MRI と有意な正の相関を示したことにより、DECT での膵実質の脂肪定量化は可能と思われた。また CT-FVF(%)と単純 100kV CT で測定した CT 値(HU)を比較すると、膵頭部と体尾部の両方で、MR-FVF(%)とCT-FVF(%)の相関はMR-FVF(%)とCT値の相関よりも良好であった。これらの結果は、DECTで測定されたCT-FVF (%)が、デュアルエネルギーモードのない従来のCT画像から得られたCT値よりも、より信頼性の高い膵臓脂肪変性の指標となる可能性を示唆している。DECTはMRIよりも撮影時間が短く、比較的簡単に撮影ができる。今後DECTが広く利用できるようになれば、膵臓脂肪定量化において実用的で非侵襲的な画像診断方法となる可能性がある。

結語:

本研究では、DECT は膵臓脂肪沈着の定量化に有用な検査法となり得ることが示された。早期の耐糖能異常の診断におけるこの技術の有用性を明らかにするためには、さらなる研究と検討が必要である。

Quantification of pancreas fat on dual energy computed tomography: Comparison with six-point Dixon magnetic resonance imaging

Abstract

Objectives: It is important to quantify the degree of fatty degeneration of the pancreas, given the reported relationship between pancreatic parenchymal fatty degeneration and pancreatic function disorder. However, it is difficult to make such a quantification using conventional computed tomography (CT). The present study evaluated the feasibility of pancreatic fat quantification by dual-energy CT (DECT) compared with T2*-corrected six-point Dixon magnetic resonance imaging (MRI).

Material and methods: Twenty-five patients who underwent both DECT (100 and 150 kVp) and Dixon MRI were analyzed. The region of interest (ROI) was placed at the head and body/tail of the pancreas on fat volume fraction (FVF) maps generated using the multimaterial decomposition (MMD) algorithm on DECT. The FVF (%) of pancreatic parenchyma measured by DECT was compared with that measured on FVF maps calculated using Dixon MRI.

Results: The median FVF (%) values of the head and body/tail of the pancreas on DECT were 8.1% (range, 1.2% - 80.9%) and 9.4% (range, 0.3% - 43.7%), respectively. The median FVF (%) values of the head and body/tail of the pancreas on Dixon MRI were 12.2% (range, 0.1% - 81.2%) and 14.2% (range, 0% - 40.8%), respectively. FVF (%) measured by DECT showed a significant correlation with the FVF (%) measured by Dixon MRI in the head of the pancreas ($r=0.894$, $P<0.001$) as well as the body/tail of the pancreas ($r=0.957$, $P<0.001$).

Conclusion: DECT may be useful for quantifying the degree of fatty degeneration of the pancreas.

Keywords:

Dual Energy Scanned Projection Radiography; Pancreas; Fats

Key points:

There have been no reports comparing advanced MRI techniques with DECT for the quantification of pancreatic fatty degeneration.

FVF (%) of the pancreas measured by DECT showed significant correlation with FVF (%) measured by Dixon MRI.

DECT may have a potential to quantify the degree of fatty degeneration of the pancreas.

Abbreviations:

DECT Dual energy computed tomography

MRI Magnetic resonance imaging

ROI Region of interest

Introdution

The accumulation of fat in the pancreas, known as pancreatic steatosis, is increasingly recognized as a cause of pancreatic dysfunction. For instance, pancreatic steatosis has been found to be associated with a decreased β-cell function and impaired insulin secretion, ultimately leading to diabetes [1-4]. Thus, it is important to quantify the degree of fatty degeneration of the pancreas reliably, noninvasively and conveniently by imaging modalities.

Magnetic resonance imaging (MRI) enables the non-invasive *in vivo* quantification of the tissue fat content [5,6]. The high accuracy of chemical shift–based MR techniques in particular, such as six-point Dixon and MR spectroscopy, for tissue fat quantification has been shown in various organs, including the liver and pancreas, in recent studies [7-10].

Although pancreatic steatosis can be visualized with computed tomography (CT), it has proven difficult to reliably quantify the tissue fat content in the pancreas using conventional CT [11,12]. However, with recent advances in dual-energy CT (DECT) technology, some studies have found that DECT with three-material decomposition was able to accurately quantify the liver fat content and could be performed on both contrast-enhanced and non–contrast-enhanced data sets [13-15]. Still, there have been no reports comparing advanced MRI techniques with DECT for the quantification of pancreatic fatty degeneration. The present study therefore evaluated the feasibility of pancreatic fat quantification by DECT in the comparison with T2*-corrected six-point Dixon MRI.

Material and methods

Study population

This retrospective study was approved by the institutional review board, and the requirement for informed consent was waived. We searched our radiology and hospital information systems to identify patients who met the following inclusion criteria: (a) patients underwent both abdominal CT and MRI between November 2017 and December 2018; (b)

CT was performed in the dual-energy mode, and MRI included six-point Dixon gradient-echo (GRE) sequences; (c) DECT was performed within 30 days of MRI. Patients with a large pancreatic tumor (n=1), a high degree of pancreatic atrophy (n=1), history of surgical resection of pancreatic tumors (n=1) or an insufficient image quality for their fat volume fraction (FVF) map (n=3) were excluded.

Ultimately, 28 patients met these criteria and formed the final study group (18 men, 10 women; age range, 49-84 years; mean age, 69.4 years). The clinical indication for MR examinations in these patients was the further evaluation of upper abdominal diseases (hepatocellular carcinoma=12, metastatic liver tumors=7, bile duct cancer=3, gallbladder cancer=3, small pancreatic lesions=2, common bile duct stone=1) suspected by ultrasound or blood examinations. Patients were required to fast for at least five hours before CT and MR examinations.

DECT

DECT was performed with a dual-source CT scanner (SOMATOM FORCE; Siemens, Forchheim, Germany) equipped with 2 x-ray tubes (tube A, low kilovoltage; tube B, high kilovoltage) in dual-energy mode, and 2 corresponding detectors were installed with an angular offset of 95°. Craniocaudal CT was performed with a dual-energy protocol (detector collimation, 128 × 0.6 mm; pitch, 0.6; gantry rotation time, 0.5 second; matrix, 512 × 512). Tube voltages were set at 100 and 150 kVp (tubes A and B, respectively), using a 0.6-mm tin filter in tube B.

Six-point Dixon MRI

MRI was conducted with a 3.0-T MR system (Magnetom Prisma; Siemens Healthcare, Erlangen, Germany) and an 18-channel body coil based on our routine abdominal protocol. Breath-hold T2*-corrected six-point Dixon T1-weighted imaging was performed to obtain fat fraction images using the following parameters: TR, 9 ms; TE, 1.12, 2.46, 3.69, 4.92, 6.15, 7.37 ms; flip angle, 4°; acquisition matrix, 111 × 160; parallel imaging factor, 2; slice thickness, 3.5 mm; field of view, 306 × 350 mm; and bandwidth, 1080 Hz/pixel. The FVF map was automatically calculated and reconstructed.

Image analyses

All images were evaluated on a picture archiving and communication system (PACS) workstation (Shade Quest, Yokogawa Medical, Tokyo) by 2 radiologists (6 and 30 years' experience) in consensus, without access to the prospective reports or any clinical information. Regions of interest (ROIs) (size, 80-100 m^2) were placed at the head and body/tail of the pancreas on FVF maps generated using a dedicated dual-energy post-processing software program (Syngo via; Siemens Healthcare) with the multi-material decomposition (MMD) algorithm on DECT by the junior radiologist to measure the FVF (%) in the pancreas and then verified for accuracy by the senior radiologist.

Effort was made to draw the ROI circles as large as possible while avoiding the pancreatic duct, vessels and retroperitoneal fat. The FVF (%) of the pancreas was also measured on FVF maps obtained by six-point Dixon T1-weighted imaging at the same location as the FVF map of DECT (Figure 1). The FVF (%) of the pancreatic parenchyma measured by DECT was compared with that measured by Dixon MRI. In addition, CT attenuation values (HU) of the pancreas were also measured on unenhanced CT images at the same location as the FVF map of DECT and compared with the FVF (%) of the pancreas.

Statistical analyses

The relationship between the FVF (%) measured by DECT and that measured by Dixon MRI was assessed using a Pearson's correlation coefficient analysis. The correlation between the FVF (%) measured by Dixon MRI and the CT attenuation value (HU) measured on unenhanced 100-kV CT was also assessed using a Pearson's correlation coefficient analysis. A p-value <0.05 was considered to indicate a statistically significant difference. All statistical analyses were conducted using the SPSS software program (version 12 for Windows; SPSS, Chicago, IL, USA).

Results

FVF maps of the pancreas were successfully obtained by both DECT and six-point Dixon MRI in all patients. The median FVF (%) values of the head and body/tail of the pancreas on DECT were 8.1% (range, 1.2%-80.9%) and 9.4% (range, 0.3%-43.7%), respectively. The median FVF (%) values of the head and body/tail of the pancreas on Dixon MRI were 12.2% (range, 0.1%-81.2%) and 14.2% (range, 0%-40.8%), respectively. The relationships between the FVF (%) measured by DECT and that measured by Dixon MRI are shown in Figure 2. The FVF (%) measured by DECT showed a significant correlation with that measured by Dixon MRI in the head of the pancreas ($r=0.894$, $P<0.001$) as well as the body/tail of the pancreas ($r=0.957$, $P<0.001$).

The median CT attenuation values (HU) of the head and body/tail of the pancreas measured on unenhanced 100-kV CT were 29.5 (range, -77.6-54.2) and 39.9 (range, -4.4-144.8), respectively. Figure 3 shows the comparison between the FVF (%) measured by Dixon MRI and the CT attenuation value (HU) measured on unenhanced 100-kV CT. There was a good correlation between the FVF (%) measured by Dixon MRI and the CT attenuation value measured on unenhanced CT in the head of the pancreas ($r=-0.960$, $P<0.001$), while the FVF (%) measured by Dixon MRI showed a weak correlation with the CT attenuation value in the body/tail of the pancreas ($r=-0.416$, $P=0.028$).

Discussion

Visceral adipose tissue is a known risk factor for the development of metabolic syndrome and cardiovascular diseases [1,2]. In the pancreas, several studies have shown that increased intrapancreatic fat is associated with type 2 diabetes [3,4] and with the exacerbation of acute pancreatitis because of its lipotoxicity [16]. Therefore, the noninvasive quantification of pancreatic fat is clinically important.

The present study showed that there was a significant positive correlation between the FVF (%) measured by DECT and that measured by Dixon MRI in the pancreas. This indicates that FVF measurement on DECT is useful for the quantification of pancreatic steatosis, since six-point Dixon MRI has been used as a highly accurate technique for quantifying fat content of abdominal organs. Notably, FVF measurement using DECT is an advanced technique that can only be applied using the latest CT systems. However, given that CT can be performed conveniently with a short acquisition time and has a higher potential throughput and better cost-effectiveness than MRI, DECT may be an extremely practical, noninvasive imaging modality for the quantification of pancreatic fat when it becomes widely available in clinical practice.

Some studies have suggested that pancreatic fat deposition might play a role in the pathogenesis of type 2 diabetes as a result of beta cell dysfunction and impaired insulin secretion [3,4,17]. In addition, pancreatic steatosis might begin with a decline in insulin secretion from the very early stage of glucose intolerance [18]. Therefore, the quantification of the severity of pancreatic steatosis by DECT will be important for the surveillance of impaired glucose tolerance, although the mechanism by which pancreatic steatosis might induce decreased insulin secretion in the early stage of the disease is not clearly understood. Further clinical studies in patients with pancreatic endocrine dysfunction as well as surveillance of impaired glucose tolerance will be necessary in order to validate the present results derived from the DECT quantification of pancreatic fat.

Several imaging modalities have been developed to assess pancreatic steatosis. Ultrasonography (US) is simple but is of limited value in the evaluation of the entire pancreas due to the location of the pancreas behind the stomach or colon [19]. In addition, US provides only a qualitative assessment of pancreatic steatosis [20]. Conventional single-energy CT has also been used to assess pancreatic steatosis. However, CT attenuation measurements are semiquantitative, with the pancreatic fat concentration merely inferred [21], and these assessments can be affected by other components in the pancreas, such as manganese [22], which can mask changes in CT attenuation induced by fatty infiltration [23].

A recent study showed that pancreatic fat measurements on unenhanced CT images and in histologic specimens obtained from pancreatectomy were significantly correlated [24]. On comparing the FVF (%) measured by Dixon MRI and the CT attenuation value (HU) measured on unenhanced 100-kV CT in this study, the FVF in the head of the pancreas correlated well with the CT attenuation value, while the FVF in the body/tail of the pancreas showed only a weak correlation with the CT attenuation value. In our study, the degree of pancreatic steatosis was relatively severe in the body/tail compared with the head of the pancreas. These results suggest that the FVF might be a more reliable indicator of pancreatic steatosis than the CT attenuation values derived from conventional CT images without a dual-energy mode.

Several limitations associated with the present study warrant mention. First, a selection bias may have been unavoidable due to the retrospective nature of this study. In addition, our study enrolled a relatively small number of patients with various pathological diagnoses, which may have been a confounding factor. Second, there was no histological correlation in the degree of pancreatic steatosis. However, several MR studies have shown the effectiveness of the Dixon MR technique for the quantification of the tissue fat content [25,26]. Third, the size of the subgroup with moderate-to-severe pancreatic steatosis (FVF ≥20%) was small. The validity of our results should be investigated in a larger cohort group involving moderate-to-severe fat infiltration of the pancreas. Fourth, regarding the ROI measurements, it would have been better to measure the FVF of the head, body and tail of the pancreas separately (three ROIs) for a more precise evaluation. However, ROI measurement from the pancreatic tail was often difficult because of age-related atrophic changes or hypoplasia.

In conclusion, DECT has potential utility for quantifying the degree of fatty degeneration of the pancreas. Further studies will be required in order to determine the usefulness of this technique for the early detection of impaired insulin secretion to prevent the development of diabetes.

References

1. Tchernof A, Despres JP (2013) Pathophysiology of human visceral obesity: an update. Physiological Reviews 93:359-404
2. Fox CS, Massaro JM, Hoffmann U et al (2007) Abdominal visceral and subcutaneous adipose tissue compartments: association with metabolic risk factors in the Framingham Heart Study. Circulation 116:39-48
3. Wong VW, Wong GL, Yeung DK et al (2014) Fatty pancreas, insulin resistance, and beta-cell function: a population study using fat-water magnetic resonance imaging. American Journal of Gastroenterology 109:589-597
4. Tushuizen ME, Bunck MC, Pouwels PJ et al (2007) Pancreatic fat content and beta-cell function in men with and without type 2 diabetes. Diabetes Care 30:2916-2921
5. Lingvay I, Esser V, Legendre JL et al (2009) Noninvasive quantification of pancreatic fat in humans. Journal of Clinical Endocrinology and Metabolism 94:4070-4076
6. Hu HH, Kim HW, Nayak KS, Goran MI (2010) Comparison of fat-water MRI and single-voxel MRS in the assessment of hepatic and pancreatic fat fractions in humans. Obesity (Silver Spring) 18:841-847
7. Kuhn JP, Hernando D, Munoz del Rio A et al (2012) Effect of multipeak spectral modeling of fat for liver iron and fat quantification: correlation of biopsy with MR imaging results. Radiology 265:133-142
8. Meisamy S, Hines CD, Hamilton G et al (2011) Quantification of hepatic steatosis with T1-independent, T2-corrected MR imaging with spectral modeling of fat: blinded comparison with MR spectroscopy. Radiology 258:767-775
9. Yokoo T, Shiehmorteza M, Hamilton G et al (2011) Estimation of hepatic proton-density fat fraction by using MR imaging at 3.0 T. Radiology 258:749-759
10. Kuhn JP, Berthold F, Mayerle J et al (2015) Pancreatic Steatosis Demonstrated at MR Imaging in the General Population: Clinical Relevance. Radiology 276:129-136

11. Kodama Y, Ng CS, Wu TT et al (2007) Comparison of CT methods for determining the fat content of the liver. AJR: American Journal of Roentgenology 188:1307-1312
12. Limanond P, Raman SS, Lassman C et al (2004) Macrovesicular hepatic steatosis in living related liver donors: correlation between CT and histologic findings. Radiology 230:276-280
13. Fischer MA, Gnannt R, Raptis D et al (2011) Quantification of liver fat in the presence of iron and iodine: an ex-vivo dual-energy CT study. Investigative Radiology 46:351-358
14. Hyodo T, Hori M, Lamb P et al (2017) Multimaterial Decomposition Algorithm for the Quantification of Liver Fat Content by Using Fast-Kilovolt-Peak Switching Dual-Energy CT: Experimental Validation. Radiology 282:381-389
15. Hyodo T, Yada N, Hori M et al (2017) Multimaterial Decomposition Algorithm for the Quantification of Liver Fat Content by Using Fast-Kilovolt-Peak Switching Dual-Energy CT: Clinical Evaluation. Radiology 283:108-118
16. Navina S, Acharya C, DeLany JP et al (2011) Lipotoxicity causes multisystem organ failure and exacerbates acute pancreatitis in obesity. Science Translational Medicine 3:107ra110
17. Heni M, Machann J, Staiger H et al (2010) Pancreatic fat is negatively associated with insulin secretion in individuals with impaired fasting glucose and/or impaired glucose tolerance: a nuclear magnetic resonance study. Diabetes/Metabolism Research and Reviews 26:200-205
18. Yokota K, Fukushima M, Takahashi Y, Igaki N, Seino S (2012) Insulin secretion and computed tomography values of the pancreas in the early stage of the development of diabetes. J Diabetes Investig 3:371-376
19. Hoff FL, H G, NA H, RM G (2008) Pancreas: normal anatomy and examination techniques. In: Gore RM, Levine MS, eds. Textbook of gastrointestinal radiology Philadelphia, Pa: Saunders:1839–1853

20. Ricci C, Longo R, Gioulis E et al (1997) Noninvasive in vivo quantitative assessment of fat content in human liver. Journal of Hepatology 27:108-113
21. Sanyal AJ (2002) AGA technical review on nonalcoholic fatty liver disease. Gastroenterology 123:1705-1725
22. Zinreich SJ, Kennedy DW, Malat J et al (1988) Fungal sinusitis: diagnosis with CT and MR imaging. Radiology 169:439-444
23. Ly JN, Miller FH (2002) MR imaging of the pancreas: a practical approach. Radiologic Clinics of North America 40:1289-1306
24. Kim SY, Kim H, Cho JY et al (2014) Quantitative assessment of pancreatic fat by using unenhanced CT: pathologic correlation and clinical implications. Radiology 271:104-112
25. Henninger B, Zoller H, Kannengiesser S, Zhong X, Jaschke W, Kremser C (2017) 3D Multiecho Dixon for the Evaluation of Hepatic Iron and Fat in a Clinical Setting. 46:793-800
26. Yoon JH, Lee JM, Lee KB et al (2016) Pancreatic Steatosis and Fibrosis: Quantitative Assessment with Preoperative Multiparametric MR Imaging. Radiology 279:140-150

Figure legends

Figure 1. Measurement of fat volume fraction (FVF) (%).

a) and b) FVF maps generated from DECT. c) and d) FVF maps obtained by six-point Dixon T1-weighted imaging. Red circles in the head and the body/tail of the pancreas represent ROIs placed for the measurement of FVF (%). ROIs were initially placed on the FVF maps of DECT, and then were placed on the FVF maps of Dixon MRI at the same location as the FVF map of DECT.

Figure 2. a) and b) The relationship between FVF (%) measured by DECT and FVF (%) measured by Dixon MRI in the head (a) and the body/tail (b) of the pancreas. FVF (%) measured by DECT showed significant correlation with FVF (%) measured by Dixon MRI in both head ($r=0.969$, $P<0.001$) and body/tail ($r=0.877$, $P<0.001$) of the pancreas.

Figure 3. a) and b) The relationship between FVF (%) measured by Dixon MRI and CT attenuation value (HU) measured on unenhanced 100kV CT in the head (a) and the body/tail (b) of the pancreas. CT attenuation value measured on unenhanced CT in the head of the pancreas showed good correlation with FVF (%) measured by Dixon MRI ($r=-0.956$, $P<0.001$) while it showed weak correlation with FVF (%) measured by Dixon MRI in the body/tail ($r=-0.416$, $P<0.05$).

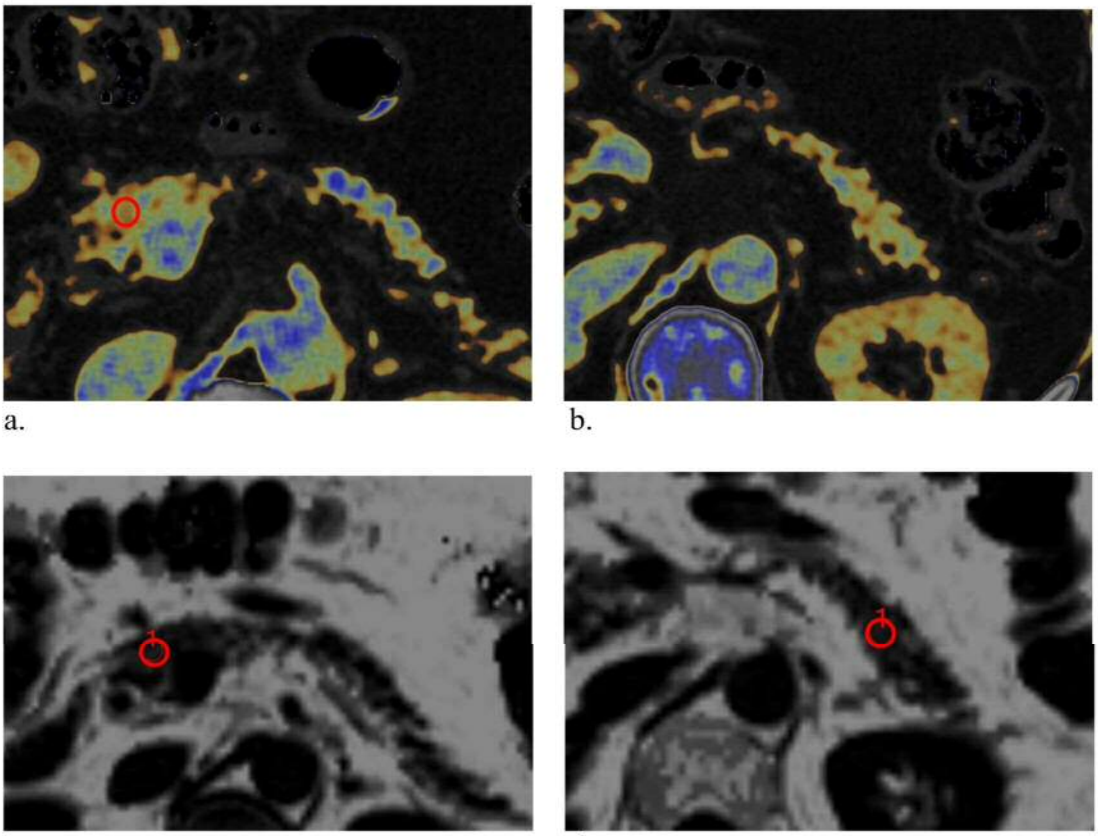

a. b. c. d.

Figure 1. Measurement of fat volume fraction (FVF) (%).

a) and b) FVF maps generated from DECT. c) and d) FVF maps obtained by six-point Dixon T1-weighted imaging. Red circles in the head and the body/tail of the pancreas represent ROIs placed for the measurement of FVF (%). ROIs were initially placed on the FVF maps of DECT, and then were placed on the FVF maps of Dixon MRI at the same location as the FVF map of DECT.

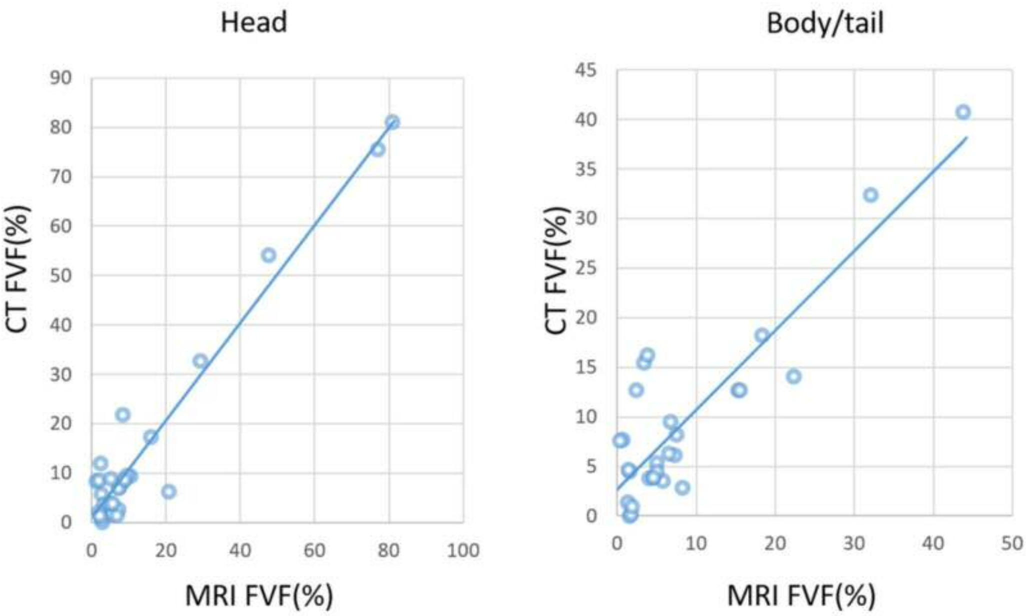

a. b.

Figure 2. a) and b) The relationship between FVF (%) measured by DECT and FVF (%) measured by Dixon MRI in the head (a) and the body/tail (b) of the pancreas. FVF (%) measured by DECT showed significant correlation with FVF (%) measured by Dixon MRI in both head ($r=0.969$, $P<0.001$) and body/tail ($r=0.877$, $P<0.001$) of the pancreas.

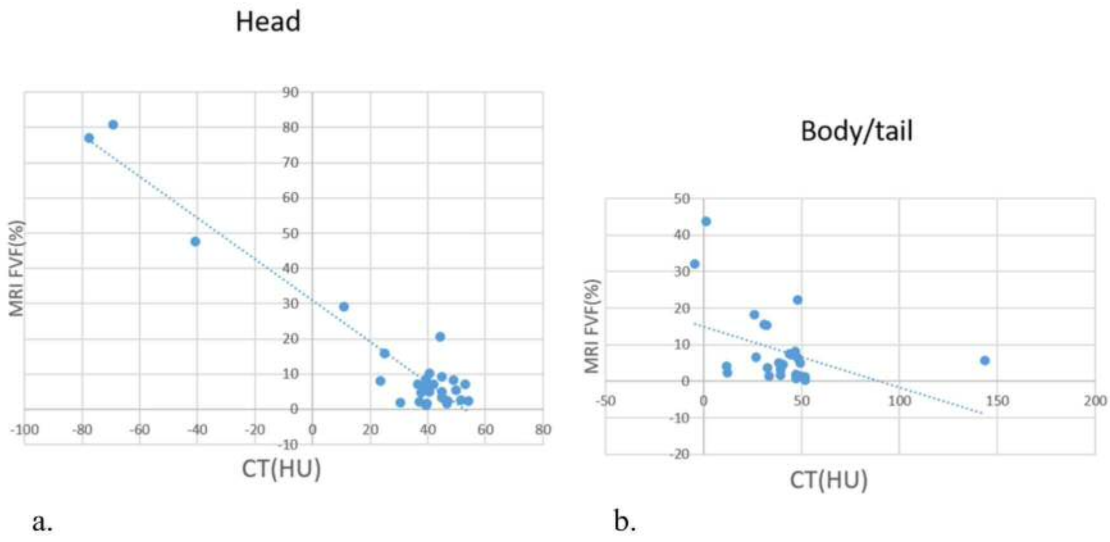

Figure 3. a) and b) The relationship between FVF (%) measured by Dixon MRI and CT attenuation value (HU) measured on unenhanced 100kV CT in the head (a) and the body/tail (b) of the pancreas. CT attenuation value measured on unenhanced CT in the head of the pancreas showed good correlation with FVF (%) measured by Dixon MRI ($r=-0.956$, $P<0.001$) while it showed weak correlation with FVF (%) measured by Dixon MRI in the body/tail ($r=-0.416$, $P<0.05$).